Effects of a Non-absorbable Gas on the Absorption Process in a Vertical Tube Absorber

Ki Joon Hur*, Eun Soo Jeong**, Si Young Jeong***

Key Words : LiBr/water, Non-absorbable gas, Absorption process, Vertical tube absorber, Heat and mass transfer

Abstract

Effects of a non-absorbable gas on the absorption process in a vertical tube absorber has been investigated numerically. The water vapor mixed with air is absorbed into LiBr/water solution film. The flow is assumed to be laminar and fully developed in both liquid and gas phases. The diffusion and energy equations were solved in both phases to give the temperature and concentrations, from which heat and mass fluxes were determined. The local absorption rate has been shown to decrease as the mass fraction of air in the water vapor increases. The vapor pressure of water at the liquid-vapor is interface reduced significantly since the non-absorbable gas accumulates near the interface. The effects of non-absorbable gases on absorption rate become larger as the mass flow rate of the vapor decreases. For a small amount of non-absorbable gases, the total absorption rate of water vapor increases as the mass flow rate of the vapor decreases. The total absorption rate increases as the mass flow rate of the vapor increases for large concentrations of non-absorbable gases at the inlet of an absorber.

Nomenclature

C : Mass concentration of LiBr
D : Mass diffusivity
g : Gravity
H_a : Heat of absorption
k : Thermal conductivity
L : Length of an absorber

* Graduate School, Hongik University, 72-1 Sangsudong, Mapoku, Seoul 121-791, Korea
** Department of Mechanical Engineering, Hongik University, 72-1 Sangsudong, Mapoku, Seoul 121-791, Korea
*** Department of Mechanical Engineering, Sogang University, 1 Sinsudong, Mapoku, Seoul 121-742, Korea

$\dot{M}_{total}$: Total absorption rate of water vapor
$\dot{m}_{abs}$: Mass flux of water vapor
p : Pressure
p_{vs} : Water vapor pressure at the liquid and vapor interface
r : Radial coordinate (Fig.1)
R : Radius of absorber tube (Fig.1)
T : Temperature
u : Axial velocity
W : Concentration of water vapor in vapor phase
W_a : Concentration of air in vapor phase
x : Axial coordinate (Fig.1)

Greek Letters

α : Thermal diffusivity
Γ : Mass flow rate
δ : Film thickness
η : Dimensionless coordinate in radial direction
μ : Viscosity
ν : Kinematic viscosity
ξ : Dimensionless coordinate in axial direction
ρ : Density

Subscripts

g : Mixed vapor of water and air
i : i-th node in axial direction
in : Absorber inlet
l : Liquid film
s : Interface between liquid film and vapor
w : Absorber wall

1. Introduction

The presence of non-absorbable gases in absorption heat pump systems degrades their performance since the non-absorbable gases accumulate near the interface between the absorbent and the absorbate where they impose a diffusional barrier to absorption. One source of non-absorbable gases is the leakage of air into sub-atmospheric components, such as the evaporator or the absorber of water-lithium bromide systems. Another common source is generation of hydrogen in water-lithium bromide systems due to chemical reactions. Hydrogen is primarily produced in the hottest component, the generator.[1,2]

Burduko vet al.[3] experimentally investigated the effect of a non-absorbable gas on the absorption of water vapor by aqueous lithium bromide flowing down a bundle of horizontal tubes. Their results indicated a 50 % reduction in mass transfer for as little as 0.5 % volumetric concentration of a non-absorbable gas. At a non-absorbable gas concentration of 2 % the reduction in mass transfer was reported to be 60 %. However, Yang and Wood[4] reported that the absorption reduction for a laminar wavy film of aqueous lithium chloride was significantly lower than that reported by Burdukov et al.[3] and that the reduction was continuous for up to 30 % volumetric concentration of air. Vliet and Cosenza[5] provided data on the effect of air on the heat and mass transfer for falling water-lithium bromide films on a vertical column of horizontal tubes. Their results showed that bulk concentrations of air below about 0.1% result in a small effect on heat and mass transfer, but that concentrations of 1% and 5% can result in degradations of about 20 % and 50 %. Son et al.[6] and Lee et al.[7] investigated the effects of non-absorbable gases on the absorption process of water vapor into water-lithium bromide solution flowing inside a vertical tube absorber experimentally.

A few existing analyses have dealt with the absorption process in presence of non-absorbable gases. Grossman[2] obtained solutions of diffusion and energy equations for both liquid and vapor phases and showed that a significant difference exists between the total absence and small presence of non-absorbable gases. Habib et al.[8] extended the work of Grossman[2] and showed a continuous reduction of absorption of absorbate with an increase in the amount of air. But, their analyses were restricted to the entrance region where an analytical solution is possible. Yang and Chen[9] presented a numerical study for simultaneous heat and mass transfer in a falling liquid film absorption process with non-absorbable gases. Their results indicated that, even with a very low percentage of ambient non-absorbable gases, the local non-absorbable gas concentration at the gas-liquid interface could be very large. Consequently, the reduction in mass absorption rate was significant. They assumed that the ambient gas flow was uniform with a velocity equal to the interface velocity and that the concentration of water vapor far from the interface was constant. Hence, their model cannot show effects of vapor velocity on the absorption process. Lee et al.(10) proposed a quasi one-dimensional model to investigate the effect of non-absorbable gases on the absorption process within a vertical tube absorber using the integral method.

In this study the effect of non-absorbable gases on the absorption process in a vertical tube absorber has been investigated numerically. The flow was assumed to be laminar and fully developed in both liquid and vapor phases. The diffusion and energy equations were solved in both phases and the mass conservations of liquid and vapor were considered. Effects of concentration of non-absorbable gases at the absorber inlet, vapor mass flow rate, and liquid mass flow rate on the absorber performance were investigated.

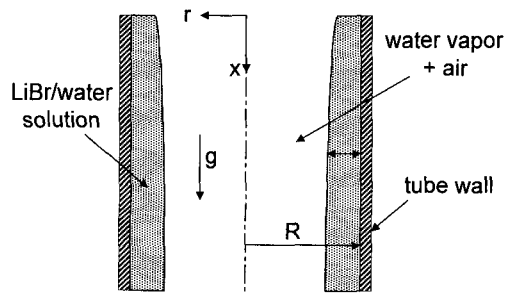

Fig.1 Schematic of a vertical tube absorber.

2. Analysis Model and Governing Equations

Figure 1 illustrates the vertical tube absorber under consideration. A film of water-lithium bromide solution flows down along an isothermal tube wall and the water vapor mixed with air flows concurrently with the liquid film. Major assumptions used in this study are as follows:

(1) The liquid and vapor flows are laminar and fully developed.

(2) The physical properties of the liquid and the vapor phases are constant.

(3) Thermodynamic equilibrium exists at the liquid-vapor interface.

(4) Heat and mass transfers occur by diffusion in the radial direction and convection in the axial direction.

Under these assumptions the momentum conservation equation of both liquid and vapor phases in the $x-$direction can be written as[11]

$$0=-\frac{1}{\rho}\frac{dp}{dx}+\nu\frac{1}{r}\frac{\partial}{\partial r}\left(r\frac{\partial u}{\partial r}\right)+g \qquad (1)$$

From the boundary conditions $u_l=0$ at

$r=R$, $u_l=u_g=u_s$ at $r=R-\delta$, and $\partial u_g/\partial r=0$ at $r=0$ the velocity profiles of the liquid and the vapor phases can be obtained as follows.

$$u_l=\frac{gR^2}{4\nu_l}\left(1-\frac{dp/dx}{\rho_l g}\right)\left[1-\left(\frac{r}{R}\right)^2-\left\{1-\left(1-\frac{\delta}{R}\right)^2\right\}\frac{\ln(r/R)}{\ln(1-\delta/R)}\right]+u_s\frac{\ln(r/R)}{\ln(1-\delta/R)} \quad (2)$$

$$u_g=\frac{gR^2}{4\nu_g}\left(1-\frac{dp/dx}{\rho_g g}\right)\left[\left(1-\frac{\delta}{R}\right)^2-\left(\frac{r}{R}\right)^2\right]+u_s \quad (3)$$

Here, subscripts l and g represent liquid and vapor, respectively. ρ is density and ν is kinematic viscosity. u_s is the velocity at the interface between the liquid and the vapor.

Since the shear stresses of the liquid and the vapor are identical at the liquid-vapor interface, the following relation can be obtained from equations (2) and (3).

$$-\frac{\rho_l gR}{4}\left(1-\frac{dp/dx}{\rho_l g}\right)\left[2\left(1-\frac{\delta}{R}\right)+\frac{1-(1-\delta/R)^2}{(1-\delta/R)\ln(1-\delta/R)}\right]+\frac{\mu_l u_s/R}{(1-\delta/R)\ln(1-\delta/R)}=-\frac{\rho_g gR}{2}\left(1-\frac{dp/dx}{\rho_g g}\right)\left(1-\frac{\delta}{R}\right) \quad (4)$$

μ_g and μ_l are liquid and vapor viscosities, respectively.

The mass flow rates of the liquid and the vapor obtained from equations (2) and (3) can be expressed as follows:

$$\Gamma_l=\frac{\pi\rho_l gR^4}{4\nu_l}\left(1-\frac{dp/dx}{\rho_l g}\right)\left[1-\left(1-\frac{\delta}{R}\right)^2-\frac{1-(1-\delta/R)^4}{2}+\left\{1-\left(1-\frac{\delta}{R}\right)^2\right\}\times\left\{\left(1-\frac{\delta}{R}\right)^2+\frac{1-(1-\delta/R)^2}{2\ln(1-\delta/R)}\right\}\right]$$

$$-\pi\rho_l u_s R^2\left[\left(1-\frac{\delta}{R}\right)^2+\frac{1-(1-\delta/R)^2}{2\ln(1-\delta/R)}\right] \quad (5)$$

$$\Gamma_g=\frac{\pi\rho_g gR^4}{4\nu_g}\left(1-\frac{dp/dx}{\rho_g g}\right)\left[\left(1-\frac{\delta}{R}\right)^4-\frac{(1-\delta/R)^4}{2}\right]+\pi\rho_g u_s(R-\delta)^2 \quad (6)$$

Under assumption (4) the governing equations of mass and heat transfer in the liquid phase can be written as[11]

$$u_l\frac{\partial C}{\partial x}=D_l\left(\frac{\partial^2 C}{\partial r^2}+\frac{1}{r}\frac{\partial C}{\partial r}\right) \quad (7)$$

$$u_l\frac{\partial T_l}{\partial x}=\alpha_l\left(\frac{\partial^2 T_l}{\partial r^2}+\frac{1}{r}\frac{\partial T_l}{\partial r}\right) \quad (8)$$

where C and T_l represent the LiBr mass concentration and the liquid phase temperature, respectively. D_l is the mass diffusivity and α_l is the thermal diffusivity of the liquid.

The governing equations of mass and heat transfer in the vapor phase can be written as[11]

$$u_g\frac{\partial W}{\partial x}=D_g\left(\frac{\partial^2 W}{\partial r^2}+\frac{1}{r}\frac{\partial W}{\partial r}\right) \quad (9)$$

$$u_g\frac{\partial T_g}{\partial x}=\alpha_g\left(\frac{\partial^2 T_g}{\partial r^2}+\frac{1}{r}\frac{\partial T_g}{\partial r}\right) \quad (10)$$

where W and T_g are the mass concentrations of water vapor and vapor temperature, respectively. D_g is the mass diffusivity and α_g is the thermal diffusivity of the vapor.

Inlet conditions and boundary conditions can be expresses as follows:

$x=0$; $T_l=T_{l,in}$, $C=C_{in}$, $T_g=T_{g,in}$, $W=W_{in}$

$r=R$; $T_l=T_w$, $\partial C/\partial r=0$

$r=0$; $\partial T_g/\partial r=0$, $\partial W/\partial r=0$

$$r=R-\delta \ ; \ T_l=T_g,$$

$$-k_l\frac{\partial T_l}{\partial r}=-k_g\frac{\partial T_g}{\partial r}+\dot{m}_{abs}H_a,$$

$$\frac{\rho_l D_l}{C_s}\frac{\partial C}{\partial r}=-\frac{\rho_g D_g}{1-W}\frac{\partial W}{\partial r} \tag{11}$$

3. Numerical Method

Since the film thickness, δ, varies along the tube as the water vapor is absorbed into the liquid film, the following coordinate transformation is used for the convenience of numerical analysis.

$$\xi=x/L \tag{12}$$

$$\eta_l=(R-r)/\delta \tag{13}$$

$$\eta_g=r/(R-\delta) \tag{14}$$

Equations (7)-(10) are transformed into(12)

$$\frac{u_l}{L}\frac{\partial C}{\partial \xi}-\frac{u_l}{L}\frac{\eta_l}{\delta}\frac{d\delta}{d\xi}\frac{\partial C}{\partial \eta_l}=D_l\left[\frac{1}{\delta^2}\frac{\partial^2 C}{\partial \eta_l^2}-\frac{1}{(R-\delta\eta_l)\delta}\frac{\partial C}{\partial \eta_l}\right] \tag{15}$$

$$\frac{u_l}{L}\frac{\partial T_l}{\partial \xi}-\frac{u_l}{L}\frac{\eta_l}{\delta}\frac{d\delta}{d\xi}\frac{\partial T_l}{\partial \eta_l}=\alpha_l\left[\frac{1}{\delta^2}\frac{\partial^2 T_l}{\partial \eta_l^2}-\frac{1}{(R-\delta\eta_l)\delta}\frac{\partial T_l}{\partial \eta_l}\right] \tag{16}$$

$$\frac{u_g}{L}\frac{\partial W}{\partial \xi}+\frac{u_g}{L}\frac{\eta_g}{R-\delta}\frac{d\delta}{d\xi}\frac{\partial W}{\partial \eta_g}=D_g\left[\frac{1}{(R-\delta)^2}\frac{\partial^2 W}{\partial \eta_g^2}-\frac{1}{(R-\delta)^2\eta_g}\frac{\partial W}{\partial \eta_g}\right] \tag{17}$$

$$\frac{u_g}{L}\frac{\partial T_g}{\partial \xi}+\frac{u_g}{L}\frac{\eta_g}{R-\delta}\frac{d\delta}{d\xi}\frac{\partial T_g}{\partial \eta_g}=\alpha_g\left[\frac{1}{(R-\delta)^2}\frac{\partial^2 T_g}{\partial \eta_g^2}-\frac{1}{(R-\delta)^2\eta_g}\frac{\partial T_g}{\partial \eta_g}\right] \tag{18}$$

Inlet and boundary conditions(equation (11)) can be rewritten as

$$\xi=0 \ ; \ T_l=T_{l,in}, \ C=C_{in}, \ T_g=T_{g,in}, \ W=W_{in}$$

$$\eta_l=0 \ ; \ T_l=T_w, \ \partial C/\partial \eta_l=0$$

$$\eta_g=0 \ ; \ \partial T_g/\partial \eta_g=0, \ \partial W/\partial \eta_g=0$$

$$\eta_l=\eta_g=1 \ ; \ T_l=T_g,$$

$$\frac{k_l}{\delta}\frac{\partial T_l}{\partial \eta_l}=-\frac{k_g}{(R-\delta)}\frac{\partial T_g}{\partial \eta_g}+\dot{m}_{abs}H_a,$$

$$-\frac{\rho_l D_l}{C_s\delta}\frac{\partial C}{\partial \eta_l}=-\frac{\rho_g D_g}{(1-W_s)(R-\delta)}\frac{\partial W}{\partial \eta_g} \tag{19}$$

Solutions of equations (15)-(18) are obtained by a finite difference method.

The mass flux of the water vapor absorbed into the liquid film can be obtained from the concentration and temperature profiles of the liquid and the vapor phases. The mass flow rates of the liquid and vapor phases at $i-$th node can be obtained from the following relations.

$$\Gamma_{l,i}=\Gamma_{l,i-1}+\frac{(\dot{m}_{abs,i-1}+\dot{m}_{abs,i})}{2}2\pi(R-\delta)\Delta x \tag{20}$$

$$\Gamma_{g,i}=\Gamma_{g,i-1}-\frac{(\dot{m}_{abs,i-1}+\dot{m}_{abs,i})}{2}2\pi(R-\delta)\Delta x \tag{21}$$

Film thickness, δ, axial pressure gradient, dp/dx, and the interface velocity, u_s, can be obtained from equations (4), (5) and (6).

A finite difference scheme marching in the ξ-direction is employed. Temperature and concentration profiles and the mass flux of the water vapor at the $i-$th node are calculated using the film thickness at the $(i-1)$th node. Newly obtained mass flux of the water vapor is used to calculate δ, dp/dx and u_s. This process is repeated until the film thickness converges.

4. Results and Discussion

Table 1 shows the dimensions and the reference operating conditions of the absorber used in this study.[13] Mass diffusivity of the vapor is obtained by the Wilke-Lee method,[14] and thermal conductivity is calculated by the method of Mason and Saxena.[15] The film thickness at the inlet for the reference operating condition is 0.44mm.

Figure 2 shows the effect of a non-absorbable gas on the absorption rate. The mass flux of the water vapor absorbed into the film decreases as the air concentration at the inlet increases. The water vapor pressure in the liquid is lower than that in the vapor since the liquid solution at the inlet is subcooled. Thus, absorption occurs at the liquid-vapor interface. As the inlet air concentration increases, the water vapor pressure in the vapor decreases. Hence, absorption rate decreases. As the water vapor is absorbed into the liquid film the interface temperature increases due to the release of absorption heat. This increases the vapor pressure in the liquid and drastically decreases the absorption rate near the inlet. After a slight increase near x=3cm the absorption rate decreases slowly because the heat transfer rate from the interface to the wall decreases as the liquid film temperature decreases.

Temperature and concentration variations in the liquid film are shown in Figs. 3 and 4. The interface temperature increases rapidly due to the absorption heat release as water vapor is absorbed into the liquid film. The interface concentration of lithium bromide is lower than the bulk concentration due to the water vapor absorption. As the interface temperature increases the interface concentration increases due to the thermodynamic equilibrium condition near

Table 1 Absorber geometry and reference operating conditions.

Parameter	Values
Absorption tube diameter(mm)	13.3
Absorption tube length(mm)	1000
System pressure(mmHg)	8.0
Wall temperature(℃)	35.0
Solution LiBr concentration(%)	58.0
Solution temperature(℃)	40.0
Solution flowrate(kg/min)	0.4
Gas flowrate(kg/min)	0.005
Gas temperature(℃)	8.0
Air concentration at inlet(%)	1.0

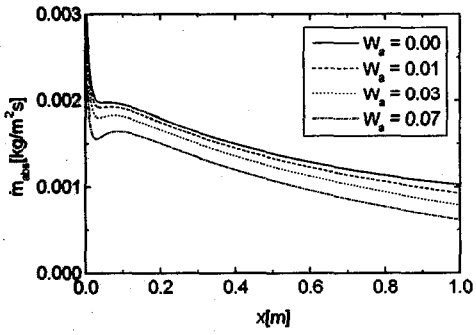

Fig.2 Effect of non-absorbable gas on local absorption rate.

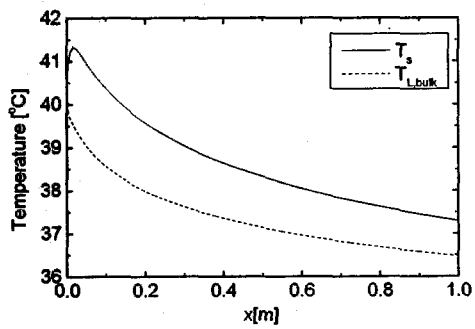

Fig.3 Bulk and surface temperature variations along the tube.

the inlet. After x=3cm, the interface temperature decreases slowly due to the cooling by the wall and the interface concentration of LiBr also decreases slowly. Both bulk temperature and bulk concentration of lithium bromide decrease slowly as the liquid flows towards the absorber outlet.

Figure 5 shows liquid and vapor temperature profiles in the radial direction. Near the inlet (x=0.001m, 0.01m) the interface temperature is higher than the inlet solution temperature due to the release of the absorption heat. The liquid film temperature decreases and the profile becomes linear as x increases. The radial temperature gradient of the vapor at the interface is large near the inlet, but it decreases slowly and the temperature of the vapor at the outlet is slightly lower than the wall temperature at the outlet.

Figure 6 shows the effect of the vapor mass flow rate on the pressure distribution within the absorber for Γ_l= 0.4 kg/min. and W_a= 0.01. Pressure decreases as x increases and the pressure drop increases as the vapor mass flow rate increases. For Γ_g= 0.006 kg/min. the pressure drop is about 10% of the inlet pressure. Therefore, the pressure drop in the absorber cannot be neglected. The pressure drop reduces the water vapor pressure in the vapor which acts as the driving potential for absorption.

The effect of the vapor mass flow rate on the absorption rate is shown in Fig.7. From the inlet to x=0.4m the absorption rate increases

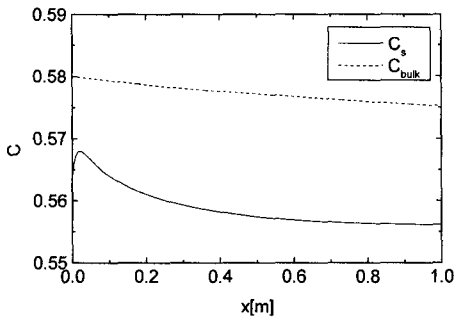

Fig.4 Bulk and surface concentration variations along the tube.

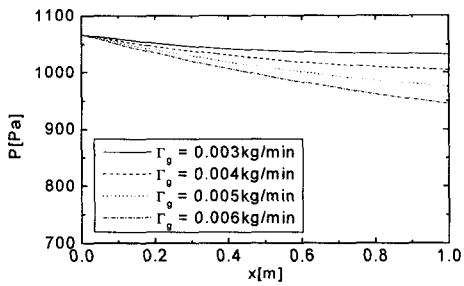

Fig.6 Effect of vapor flow rate on pressure. (Γ_l=0.4kg/min, Wa=0.01)

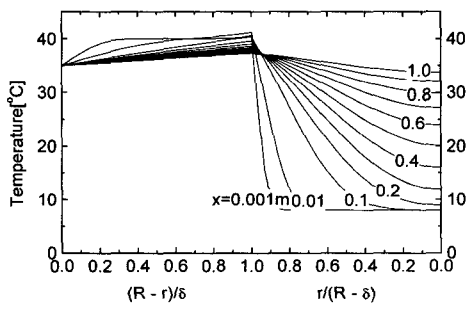

Fig.5 Variations of solution film and gas temperature profiles.

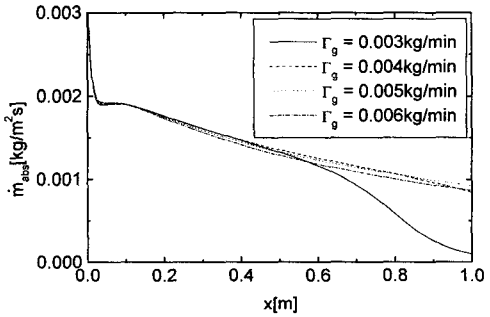

Fig.7 Effect of vapor flow rate on local absorption rate.(Γ_l=0.4kg/min, Wa=0.01)

as the vapor mass flow rate decreases. The absorption rate for Γ_g= 0.004 kg/min. is lower than that for Γ_g= 0.005 kg/min. for x> 0.8m, and the absorption rate for Γ_g= 0.003 kg/min. is drastically reduced for x> 0.5m.

Figure 8 shows the effect of the vapor mass flow rate on the partial pressure of the water vapor at the liquid-vapor interface. The advection of the vapor phase toward the interface carries non-absorbable gases with it. Since the non-absorbable gases are not absorbed into the liquid film, the partial pressure of the water vapor at the interface is reduced. The partial pressures of the water vapor near the inlet for small vapor mass flow rates are higher than those for a large vapor mass flow rates since the pressure drop for a small vapor mass flow rate is smaller than that for a large vapor mass flow rate. For a large vapor mass flow rate(Γ_g=0.005 and 0.006kg/min.) the decreasing rate of the partial pressure is almost constant near the outlet, but the partial pressure for a small vapor mass flow rate decreases significantly near the outlet. The partial pressure profiles of the water vapor at the interface are similar to those of the absorption rates shown in Fig.7 except near the entrance region. This result shows that the water vapor pressure in the vapor phase is the driving potential of the absorption.

Figure 9 shows the effects of the vapor mass flow rate and the inlet concentration of the air on the total absorption rate. For a pure water vapor flow, the total absorption rate decreases as the vapor mass flow rate increases since the pressure drop increases as the vapor mass flow rate increases. For Γ_g=0.003 kg/min. all of the water vapor entering the absorber is absorbed to the liquid film inside the absorber. For W_a=0.07, an increase of Γ_g from 0.003 kg/min. to 0.004 kg/min. results in about 13% increase of the total absorption rate. The reduction of the total absorption rate by non-absorbable gases reduced as the vapor mass flow rate decreases.

The effects of solution mass flow rate and the inlet concentration of air are shown in Fig.

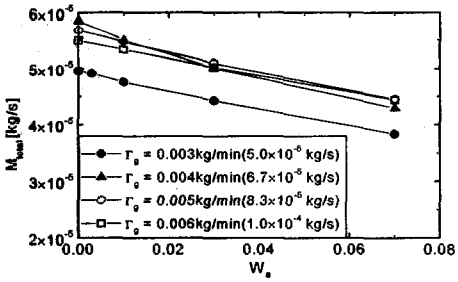

Fig.9 Effect of vapor flow rate on total absorption rate. (Γ_l=0.4kg/min)

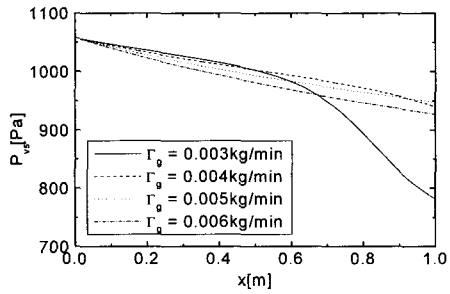

Fig.8 Effect of vapor flow rate on surface vapor pressure. (Γ_l=0.4kg/min, Wa=0.01)

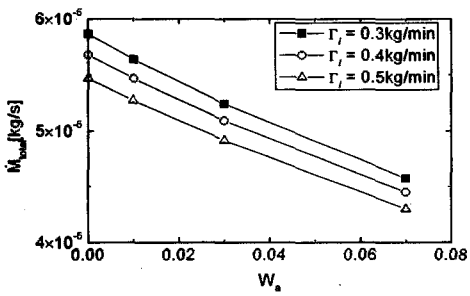

Fig.10 Effect of liquid flow rate on total absorption rate. (Γ_g=0.005kg/min)

10. As the solution mass flow rate increases, the film thickness increases and the heat transfer rate from the interface to the wall decreases. Hence, the mass flux of the water vapor absorbed into the liquid film decreases. The total absorption rate decreases almost linearly as the inlet concentration of air increases.

5. Conclusions

The absorption process within a vertical tube absorber in the presence of non-absorbable gases was investigated numerically. Pressure drop was calculated assuming that the liquid solution and the vapor phase are fully developed laminar flow. Conservation equations of mass transfer and heat transfer were applied to both liquid and vapor phases. The effects of inlet concentration of non-absorbable gas, vapor mass flow rate, and liquid mass flow rate on the absorption rate were shown.

As the inlet concentration of the non-absorbable gas increases the absorption rate decreases. Since non-absorbable gases accumulate near the liquid-vapor interface, the partial pressure of the water vapor decreases significantly and the local absorption rate is reduced near the outlet of the absorber when the vapor mass flow rate is small.

The total absorption rate due to the non-absorbable gas decreases as the vapor mass flow rate decreases. For a low inlet concentration of the non-absorbable gas the total absorption rate increases as the vapor mass flow rate decreases, but the total absorption rate increases as the vapor mass flow rate increases for a high inlet concentration of the non-absorbable gas.

6. References

(1) Vliet, G. C. and Chen, W, 1993, "Location of Non-Absorbable Gases in a Simplified Absorber Geometry," *International Absorption Heat Pump Conference*, pp. 171-177.

(2) Grossman, G., 1990, "Film Absorption Heat and Mass Transfer in the Presence of Non-Condensables," *Proceedings of the Ninth International Heat Transfer Conference*, Jerusalem, Israel, Vol. 6, pp. 247-252.

(3) Burdukov, A. P., Bufetov, N. S., Deriy, N. P., Dorikhov, A., and Kazakov, V. I., 1980, "Experimental Study of the Absorption of Water Vapor by Thin Films of Aqueous Lithium Bromide," *Heat Transfer-Soviet Res.*, Vol. 12, pp. 118-123.

(4) Yang, R. and Wood, B. D., 1988, "Heat and Mass Transfer in Laminar Wavy Film Absorption with the Presence of Non-Absorbable Gases," *Proceedings of the National Heat Transfer Conference*, Houston, 2Texas, HTD-96, Vol. 3, pp. 141-148..

(5) Vliet, G. C. and Cosenza, F. B., 1991, "Absorption Phenomena in Water-Lithium Bromide Films," *Proceedings of Absorption Heat Pump Conference*, pp. 53-61

(6) Son, B. H. and Kim, B. J., 1994, "Effects of Non-absorbable Gas on Absorption Process," *Proceedings of the Winter Meeting of Society of Air-Conditioning and Refrigerating Engineers of Korea*, pp. 7-12.

(7) Lee, C. W., Son, B. H. and Kim, B. J., 1995, "Experimental Investigation for the Effect of Non-absorbable Gases in the Absorption Process of Water Vapor into LiBr-Water Solution Flowing inner Vertical Tubes, " *Proceedings of the Winter Meeting of Society of Air-Conditioning and Refrigerating Engineers of Korea*, pp. 324-329.

(8) Habib, H. M., Ameel, T. A. and Wood, B. D., 1991, "Effects of a Non-Absorbable Gas on the Heat and Mass Transfer for the

Entrance Region of a Falling Film Absorber," *Proceedings of the JSME/ASME Thermal Engineering Conference*, Reno, Nevada, pp. 475-481.

(9) Yang, R. and Chen, J. H., 1991, "A Numerical Study of the Non-Absorbable Effects on the Falling Liquid Film Absorption," *Warme und Stoffubertragung*, Vol. 26, pp. 219-223.

(10) Lee, C. W. and Kim, B. J., "Analytical Model for the Absorption Process of Falling Film in the Presence of Non-Absorbable," *Proc. of the 3rd KSME-JSME Thermal Engineering Conf.*, 1996, pp. 541-546.

(11) Bird, R. B., Stewart, W. E., and Lightfoot, E. N., 1960, *Transport Phenomena*, John Wiley & Sons, Inc., p. 85, p. 319, p. 559.

(12) Myung, H. K., 1995, *Computational Fluid Dynamics for Engineering*, Hanmi, pp. 171-176.

(13) Kim, B. J and Lee, C. W., 1998, "Effects of Non-absorbable gas on the Absorption Process of Aqueous Lithium Bromide Solution in a Vertical Tube," *Korean Jouranl of KSME Journal(B)*, Vol. 22, No. 3, pp. 1304-1314.

(14) Treybal, R. E., 1987, *Mass-Transfer Operation*, McGraw-Hill, pp. 31-32.

(15) Reid, R. C., Prausnitz, J. M., and Poling, B. E., 1988, *The Properties of Gases & Liquids, McGraw-Hill*, pp. 530-531.